Thickness dependence of the total magnetic moment per atom in the Cu/Ni/Cu/Si(001) system

S. Hope, J. Lee, P. Rosenbusch, G. Lauhoff, J. A. C. Bland, and A. Ercole
Cavendish Laboratory, University of Cambridge, Cambridge CB3 OHE, United Kingdom

D. Bucknall and J. Penfold
Rutherford Appleton Laboratory, Chilton OX11 OQX, United Kingdom

H. J. Lauter, V. Lauter, and R. Cubitt
Institut Laue-Langevin, Avenue des Martyrs, Grenoble 38042, France
(Received 6 August 1996; revised manuscript received 29 January 1997)

Systematic measurements of the magnetic moment per Ni atom in Cu/Ni/Cu/Si(001) structures have been made using polarized neutron reflection (PNR) for Ni thicknesses in the range $30\,\text{Å} < t < 400\,\text{Å}$ at room temperature. We find a dramatic reduction in the magnetic moment per atom for $t < 100\,\text{Å}$ and near bulk values above 100 Å. These results are corroborated by alternating gradient magnetometer measurements on the same samples. A Cu/Ni-wedge/Cu/Si(001) structure with $30\,\text{Å} < t < 150\,\text{Å}$ was studied using magnetic circular x-ray dichroism (MCXD), polar magneto-optical Kerr effect (MOKE), and reflection high-energy electron diffraction (RHEED) in order to estimate the variation in the values of $\langle L_z \rangle$, $\langle S_z \rangle$, perpendicular anisotropy strength, and surface in-plane Ni lattice constant, respectively, during epitaxial growth. RHEED measurements show that the in-plane lattice constant falls by 1.7% in the Ni thickness range $30\,\text{Å} < t < 90\,\text{Å}$. The MCXD measurements reveal the same trend for $\langle L_z \rangle$, $\langle S_z \rangle$, and total moment per atom versus Ni thickness as found for the total moment by PNR. Polar MOKE measurements confirmed the transition from a perpendicular easy axis towards an in-plane magnetic easy axis as has already been extensively studied in the literature. Comparison of the PNR results with RHEED measurements reveal a striking correlation between the increase of in-plane strain and reduction in magnetic moment per atom with decreasing Ni thickness. While a direct strain-induced variation of the moment based on bulk phase calculations cannot account for the magnitude of the moment variations we observe, we show that the results cannot be attributed to sample contamination, interdiffusion, or a reduction of the Curie temperature with decreasing Ni thickness. Furthermore, the presence of a magnetically dead layer in the samples is not consistent with the PNR results. The strong moment variation partially explains the large thickness range for which perpendicular anisotropy is observed in this system. [S0163-1829(97)15317-6]

I. INTRODUCTION

In recent years many experimental studies have explored the thickness dependence of the magnetic anisotropy, magnetic order, domain structure, and Curie temperature in the Ni/Cu(001) system.[1–5] The Curie temperature of the Ni/Cu system is known to be below room temperature for thin Ni films below about five monolayers (5 ML) and to exhibit an in-plane magnetic easy axis for thicknesses of 5–9 ML (8.8–15.8 Å).[6] For larger Ni thicknesses up to 100 Å, a perpendicular magnetic anisotropy again develops as is now well known.[1–3] Ultrathin Ni films grown epitaxially on Cu(001) have an in-plane lattice constant expanded by 2.5% to match that of the Cu seed layer. This results in a corresponding tetragonal contraction in the perpendicular lattice spacing, thus causing a strain-induced magnetoelastic (ME) perpendicular anisotropy. As the Ni film grows thicker still, the magnetic easy axis returns to the in-plane direction as the shape anisotropy of the sample becomes dominant. The ME contribution of the tetragonal distortion has been calculated by Naik *et al.*[1] using lattice spacing measurements performed by Chang[3] and found to be large enough to account for the perpendicular anisotropy field. To understand the origin of the magnetic properties further, it is, however, desirable to know the magnetic moment per atom to a high precision since this is one of the most fundamental quantities. Also, the magnetization determines the demagnetizing field value $\mu_0 M$ and so the critical thickness up to which perpendicular magnetic anisotropy (PMA) can dominate. Marcus *et al.* have carried out theoretical calculations on the volume dependence of the magnetic moment per atom in various transition metals including fcc Ni.[7] However, to our knowledge the strain dependence of the magnetic moment per atom has not been systematically studied and an investigation of the Ni/Cu system provides an excellent opportunity to do this because of the large internal strains in the system identified from the magnetic anisotropy studies.

Calculations of the electronic and magnetic structure of ultrathin epitaxial films using recently developed spin-resolved band-structure techniques[8] demonstrate that the reduced atomic coordination, modified volume per atom, and the interface-induced electronic states all strongly affect the magnetic moment. Enhanced total moments[9–11] and enhanced orbital moments in systems which exhibit PMA (Refs. 12 and 13) have been reported. A reduced spin moment for one monolayer of Ni on Cu(100) has also recently

been calculated.[11] In this paper we will discuss the results of polarized neutron reflection (PNR) measurements of the absolute moments per atom on a series of samples of nominal structure Cu 50 Å/Ni/Cu 600 Å/Si(001) for Ni thicknesses in the range $30 \text{ Å} < t < 400 \text{ Å}$. The procedure for fitting the PNR data is discussed in detail and the results compared with those carried out on the same samples using conventional magnetometry [alternating gradient force magnetometry (AGFM)]. Magnetic circular x-ray dichroism (MCXD) and polar magneto-optical Kerr effect (MOKE) experiments were carried out on a wedge sample of nominal structure Cu 30 Å/Ni(30–150 Å)/Cu 600 Å/Si(001). These experiments allowed us to study the variation of $\langle L_z \rangle$ and $\langle S_z \rangle$ and anisotropy strength as a function of Ni thickness on the same sample and to compare our findings with the absolute moments as determined by PNR.

II. POLARIZED NEUTRON REFLECTION

Polarized neutron reflection is able to yield the absolute value of the magnetic moment per atom in a magnetic thin film system with high accuracy[14] and, in contrast to superconducting quantum interference device (SQUID) magnetometry, has the advantage of having no magnetic signal from the substrate requiring correction to the data. Furthermore, since SQUID magnetometry measures the total moment of a thin film sample, to calculate the magnetic moment per atom requires that the sample area and thickness be known to a high accuracy. PNR avoids this difficulty since it is, in principle, a self-calibrating magnetometric technique, allowing not only a direct measurement of the magnetic moment, but also a precise measurement of the layer thicknesses. It is a powerful technique, able to directly probe the layer-dependent magnetization vector profile in a magnetic medium.[15–17] Experimentally, polarized neutrons with spins parallel and antiparallel to the sample magnetization are reflected off the surface of the sample at grazing incidence. The potential energy of a neutron in the αth region of the sample is given by[14,15]

$$V_\alpha = \frac{2\pi\hbar^2}{m_n}\rho_\alpha b_\alpha - \boldsymbol{\mu}_n \cdot \mathbf{B}_\alpha, \qquad (1)$$

where $\boldsymbol{\mu}_n$, b_α, $\mathbf{B}_\alpha$, and ρ_α are the neutron moment, coherent nuclear scattering length, magnetic field (due to the magnetization in the region), and atomic density, respectively. This potential gives rise to a spin-dependent reflectivity which depends on the relative orientation of the spin of the incident neutron and the magnetization of each magnetic layer. The specularly reflected neutron intensity is measured as a function of the incident spin state and incident wave vector. Such measurements permit the refractive index profile of the solid medium to be determined with a depth resolution typically in the nm range. Since the strength of the Zeeman interaction is determined by the magnetic induction **B** only (the neutron moment is known), the total magnetic moment per atom (spin and orbital components) can be accurately obtained for a magnetically saturated thin ferromagnetic film of known density. By comparing the results of experiment with simulations, we can obtain information about the absolute moment per atom and the thickness of the

TABLE I. Structural and magnetic parameters of the eight samples investigated with PNR. The second column indicates the nominal thicknesses of the Ni films as given by a quartz microbalance. Columns 3 and 4 give the Ni thickness and Ni moment per atom as determined by the PNR fits. The last column is the average of the roughness values for each of the several interfaces within a given sample.

Sample	Ni thickness nominal (Å)	Ni thickness PNR (Å)	Ni moment μ_B	Interface roughness (Å)
1 (RAL)	30	30.1±3.4	0.1 ±0.09	19.5
2 (RAL)	60	53.6±3.5	0.25±0.03	13.5
3 (RAL)	80	69.6±4.5	0.23±0.05	14.7
4 (RAL)	100	78.4±4.4	0.41±0.04	10.3
5 (RAL)	150	98.1±4.1	0.63±0.03	15.0
6 (ILL)	100	103.3±6.2	0.62±0.05	22.5
7 (RAL)	300	233.9±3.8	0.57±0.02	19.4
8 (RAL)	400	373.6±11.2	0.59±0.04	18.5

magnetic and nonmagnetic layers. The difference between the spin-up and spin-down reflectivities, or spin asymmetry, gives information on the magnetic moment, while the period and detailed wave-vector dependence of the reflectivity oscillations give us information on the thickness and structure of the sample layers. The numerical technique of extracting magnetic moments from the measured spin asymmetry is by now well established and is discussed in numerous references.[14,15]

The PNR experiments were carried out on the CRISP time-of-flight neutron reflectometer at the Rutherford Appleton Laboratory (RAL) and on the D17 fixed-wavelength reflectometer at the Institut Laue-Langevin (ILL) at Grenoble. The details of the experimental setup of the two reflectometers is described elsewhere[18,15] and so will not be discussed here. The samples were subjected to a field of $H = 6$ kOe directed in the plane of the film. MOKE measurements with an in-plane applied field showed that a field of 6 kOe was sufficient to saturate 30 Å Ni. The sample sizes were approximately 1.5×1.0 cm^2. Simulations were performed using a downhill simplex numerical recipe. The same samples (cut into 2-mm^2 pieces) were then measured using an AGFM with a sensitivity in the 10^{-8}-emu range.

III. EXPERIMENTAL DETAILS

The eight samples grown for the PNR experiments were grown at room temperature and prepared in two different growth chambers. Either Knudsen cell sources or e-beam evaporation sources were used to grow the Ni films in UHV. All Cu layers were grown using e-beam evaporation. Table I gives information on the nominal structures of the eight samples as well as the sample parameter results as given by PNR. Si(001) substrates were degreased, etched in diluted HF solution for 12 min, and pull dried prior to loading into the growth chamber. The Ni was grown at 3 Å/min and at a deposition pressure of 2×10^{-9} mbar for e-beam evaporation and 5 Å/min at 3×10^{-8} mbar from the Knudsen cell. The Cu was grown at 10 Å/min at a pressure of 2×10^{-9} mbar. A wedge sample Cu 30 Å/Ni(30–150 Å)/Cu
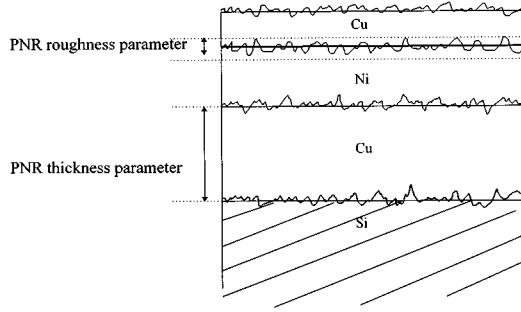
FIG. 1. Schematic diagram of the sample model used to fit the PNR data.

600 Å/Si(001) was also grown for the purposes of MCXD measurements. Both Ni and Cu were grown at room temperature. Reflection high-energy electron diffraction (RHEED) was used to confirm the epitaxial growth of Ni and Cu, and the substrate and film purity were monitored using Auger electron spectroscopy (AES). The sample thickness was monitored using a quartz microbalance, but PNR was used to give a more accurate estimation of the true magnetic thickness.

The MCXD experiment was performed at the beam line 1.1 of Daresbury Laboratory UK.[19] The sample was subjected to a field of 1 T perpendicular to the film to ensure saturation. Polar MOKE measurements were performed at room temperature using a conventional polar MOKE arrangement.[20,21] The change with applied field in the intensity of light transmitted through an analyzing polarizer (set close to extinction) after reflection from the sample (Kerr intensity) can be related to the magneto-optic Kerr rotation. RHEED measurements were performed as the wedge was grown to study the change of in-plane lattice parameter of the Cu buffer and Ni layer with thickness.

To fit the PNR experimental data, a choice has to be made as to how we model the sample in the computer simulations. Figure 1 shows schematically the model adopted in our work and from which the best fits were obtained. We assumed as constants in the fits appropriate (bulk) density and coherent scattering lengths of the individual layers. Only the magnetic moment, layer thicknesses, and interface roughness parameters are varied. There are, of course, possible alternatives to the model we have adopted. For instance, NiCu or even NiO alloy layers (representing intermixing and contamination effects at the interfaces, respectively) could be introduced between the Ni/Cu interfaces in the model of Fig. 1. In our analysis, these alternative models have proved unsuccessful in modeling the Ni/Cu data and would seem to indicate that the presence of intermixing/contamination surfaces is not significant, as we shall discuss later.

In the model we have adopted, the PNR best-fit thickness parameter is an average value, since it is assumed that there is a region of roughness associated with each interface. It is important to understand the meaning of the roughness parameter and its effect on the fitting process for our samples. In practice, defects, steps, interdiffusion, intermixing, and local fluctuations[22] in the interface position can all contribute to an effective interface roughness. Roughness has the effect of reducing the specularly reflected intensity due to diffuse scattering of some of the neutrons out of the specular beam.

The fitting program takes into account the reduction in specular intensity by introducing a multiplicative exponential factor, as proposed by Nevot and Croce[22] and given by

$$R_m = R_0 e^{-4q_1 q_2 z^2}, \tag{2}$$

where z is the root-mean-square roughness amplitude of the surface and q_1 and q_2 are the perpendicular wave vectors in media 1 and 2 bounding the interface. R_0 is the Fresnel intensity reflection coefficient for a perfectly smooth surface, and R_m is the measured specular intensity. The roughness parameters of samples 1–8 are given in Table I. A roughness amplitude z is obtained for each of the several interfaces in a given sample. These values of z are then averaged to give the values shown in the last column of Table I. The roughness parameter is the last variable to be fitted and allows a ''fine-tune'' to the best fit. The moment and thickness parameters are fitted separately, then simultaneously until a best fit is approached. Fitting the roughness parameter allows us to close in on a best fit without causing a significant change in the moment and thickness values already reached. The spin asymmetry (defined below), which is less sensitive to z^2 than the reflectivity, was also fitted for each sample.

IV. RESULTS

Representative PNR results are shown in Figs. 2(a) and 2(b) for samples 2 and 7 (see Table I). Both the reflectivity and spin asymmetry are shown for samples 2 and 7 and are plotted as a function of the reduced wave vector q/q_c where q_c is the critical wave vector below which there is total reflection from the sample surface. For the Cu/Ni/Cu/Si(001) system, $2q_c = 0.018$ Å^{-1} in units of momentum transfer (where $h/2\pi$ is conventionally taken as unity). The spin asymmetry is given by

$$S = \frac{R_\uparrow - R_\downarrow}{R_\uparrow + R_\downarrow}, \tag{3}$$

where $R_\uparrow$ and $R_\downarrow$ indicate the reflectivities of the neutrons with spins parallel (spin up) and antiparallel (spin down) to the film magnetization, respectively.

The key observation from Fig. 2 is the decreasing maximum flipping ratio ($R_\uparrow / R_\downarrow$) from sample 7 to sample 2. This behavior indicates that the difference between the potentials of the spin-up and spin-down neutrons in the Ni layer is decreasing with decreasing Ni thickness, and hence, from Eq. (1), the magnetic moment per atom in the Ni layer is decreasing. Referring to Table I, sample 1 (30 Å Ni) is surprisingly almost ''magnetically dead,'' with the moment increasing rapidly, reaching the bulk value at approximately 100 Å. To ensure the in-plane 6-kOe field applied during the PNR measurements was sufficient to saturate all of the samples, a polar MOKE measurement was carried out on a Cu 30 Å/Ni 30 Å/Cu 600 Å/Si(001) film with an in-plane applied field. Figure 3 shows the result of this measurement. At remanence the film shows a magnetization perpendicular to the film plane. This is because up and down domains will not reform in equal volumes if there is even the smallest misalignment of the in-plane applied field. Applying an in-plane field forces the magnetization into the plane of the film and the polar Kerr intensity is observed to drop to zero. From
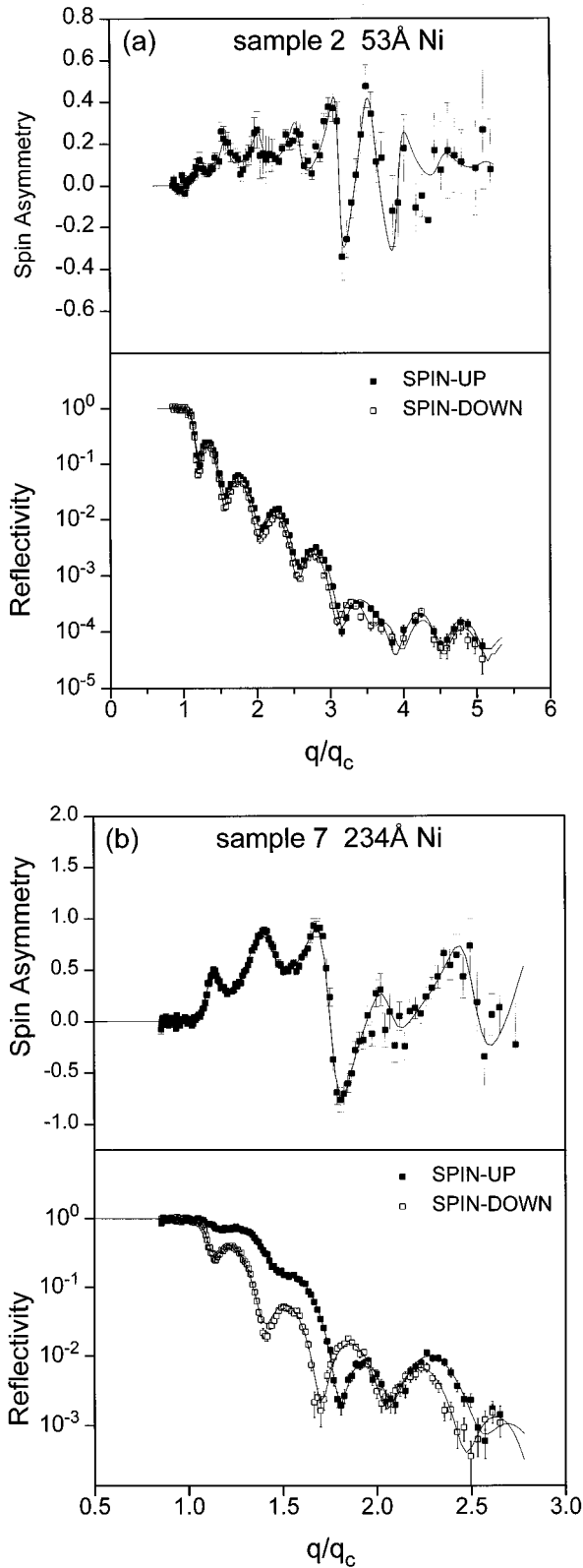
FIG. 2. Representative PNR data (symbols) and best-fit reflectivity and spin asymmetry curves (solid lines) for two samples of different thicknesses: (a) sample 2 (53 Å Ni, RAL) and (b) sample 7 (234 Å Ni, RAL). It is clear that the maximum flipping ratio $(R_\uparrow/R_\downarrow)$ is decreasing from sample 7 to 2. This indicates that the magnetic moment per atom of the Ni is decreasing for decreasing Ni thickness. Table I gives information on the best-fit parameters for the figures shown.
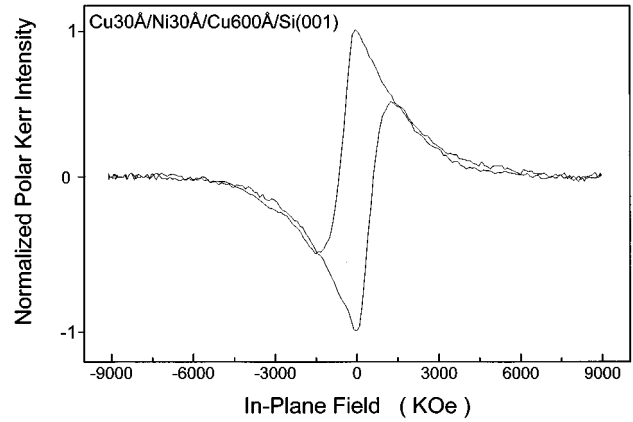

FIG. 3. Polar MOKE loop for Cu 30 Å/Ni 30 Å/Cu 600 Å/Si(001). The polar Kerr intensity is measured as a function of an in-plane applied field. At remanence, the film shows a magnetization perpendicular to the film plane. Applying an in-plane field forces the magnetization into the plane of the film, reducing the measured Kerr intensity to zero. Above 6 kOe no perpendicular component is observed, showing that 6 kOe is sufficient to saturate the samples used in this study.

Fig. 3 it is clear that no perpendicular magnetization component remains after the in-plane applied field is raised above 6 kOe and therefore 6 kOe is stronger than the perpendicular anisotropy field of the sample, and so all moments are aligned in-plane. Since all of the moments are aligned in-plane, PNR is able to accurately determine the average absolute moment per atom. We conclude that all of our samples are saturated (in plane) at the fields used during the PNR measurements. This follows because the perpendicular anisotropy field is strongest for the 30-Å Ni sample (sample 2).

It is clear that there are excellent fits to both the spin asymmetry and reflectivity data for the data in Fig. 2, highlighting the power of the technique in determining thicknesses and magnetic moments. Since we were principally concerned here with the variation of the magnetic moment with thickness rather than the detailed wave-vector dependence of the reflectivity, measurements were made only up to $2.5q_c$. Taking measurements at a higher q value than this would not have significantly improved our estimates of the layer averaged moment per atom, but higher q measurements yield more details on the variation of the magnetization within the sample. However, it is important to check that the experimental data can still be fitted at higher q values in order to establish confidence in the parameters fitted from the lower q data. To this end sample 2 (53 Å Ni) was measured up to $5q_c$. Figure 2(a) indicates that an excellent fit can still be obtained when measurements are taken to higher q. By fitting the data of sample 2 in the low-q range only and comparing the best-fit parameters with those gained from fitting the data over the entire q range, it was found that there was no significant difference in any of the parameters, thus establishing confidence in the information obtained from the low-q measurements.

As a further test of the PNR "best fits," we can compare two measurements of the same sample under different conditions in the following way. If we measure the reflectivity curves for a sample which is magnetically saturated, then we know that the moments are fully aligned and we can thus
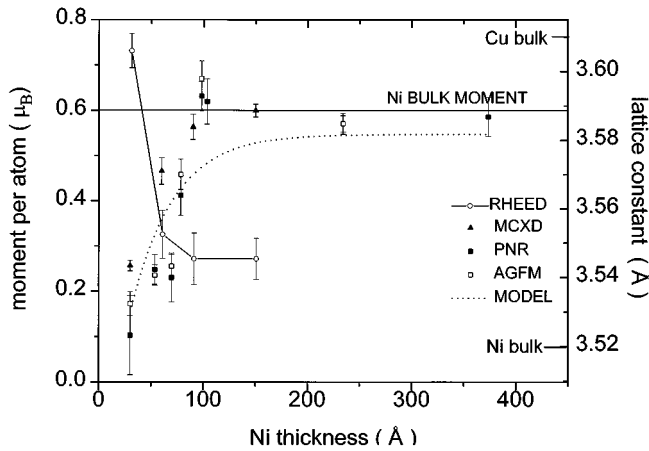
FIG. 4. Magnetic moment per atom as a function of Ni thickness as given by PNR, AGFM, and MCXD. The dotted line indicates a hypothetical model in which the Ni contains a 23-Å ''magnetically dead'' layer in the Ni. The MCXD data points refer to nominal Ni thicknesses, whereas the PNR and AGFM data points refer to thicknesses as determined by PNR. Also shown on the same scale is the change in surface in-plane lattice constant for Ni over the same thickness range. The solid line is a guide to the eye. A striking correlation between an increase of the surface Ni in-plane lattice constant and reduction in moment per atom is clearly visible.

obtain good estimates of the thickness and roughness parameters. If our best-fit thickness and roughness parameters are correct, then we should be able to use exactly the same values to fit the same sample measured at remanence, allowing only the moment to vary. The moment would change because PNR is only sensitive to the component of the moment parallel to the incoming neutrons and at remanence the formation of domains in various directions would reduce the measured layered averaged moment per atom. The long coherence length of the neutron beam projected in the plane of the film ensures that the magnetization probed corresponds to a coherent average over the domains which form within the film.[15] All of our samples were tested in this way to confirm the best-fit structural parameters in each sample. Importantly, we found that it was not possible to achieve better fits to the remanence data by further adjusting the structural parameters so justifying this method.

Figure 4 shows the variation in moment with thickness for all eight samples, and Table I gives further information on the best-fit parameters.[23] The AGFM measures the relative total moments of the samples. By measuring the area of the samples and using the thickness values obtained from PNR fits, we were able to calculate the relative moments per atom (assuming constant densities). To compare absolute moments for the two techniques, it was assumed that sample 7 (233 Å Ni) had reached the bulk value for the magnetic moment for Ni ($0.6\mu_B$). The other samples were then rescaled accordingly to give the absolute values as shown in Fig. 4. We emphasize that AGFM cannot yield the absolute moment per atom. Only PNR provides information on both the thickness and magnetization of the sample, thus providing an absolute estimate of the Ni moment per atom. Clearly, the sharp reduction in moment per atom below 100 Å is also corroborated by AGFM measurements on the same samples. There is complete agreement between the two techniques within

experimental error. Surprisingly, the PNR and AGFM results also show a slight peak in the curve at about 100 Å which might indicate a small enhancement in the moment per atom as compared to the bulk value. However, the error bars are too large to confirm this and more detailed experiments in this region with better statistics would be needed to see if this is a real effect or not.

The details of the MCXD experiment are described separately[19] and so will only be discussed in summary here. The values for both $\langle L_z \rangle$ and $\langle S_z \rangle$ were found to increase from 30 to 150 Å following the same trend as the PNR data. Although there is now wide agreement that the ratio $\langle L_z \rangle / \langle S_z \rangle$ can be measured accurately using MCXD, applying the sum rules in determining the absolute values of $\langle L_z \rangle$ and $\langle S_z \rangle$ is still contentious[24,25] and we will not try to compare the absolute moments from PNR and MCXD quantitatively. The details of how the absolute moments were calculated from the MCXD data are discussed in Ref. 19, but here we are concerned with the qualitative trends of $\langle L_z \rangle$ and $\langle S_z \rangle$. Figure 4 also shows the total moment estimated from the MCXD data following the same trend as the PNR and AGFM results. It must be emphasized here that the MCXD data points refer to nominal thicknesses, whereas the PNR and AGFM data points refer to thicknesses as measured by PNR. We have also shown on the same graph the change in surface in-plane lattice parameter for the Ni layer in the wedge sample. It is evident that there is a strong correlation between the decrease in moment per atom determined by PNR, AGFM, and MCXD and the increase in surface Ni nearest-neighbor distance determined by RHEED and, therefore, the strain in the Ni layer. The RHEED study showed three-dimensional epitaxial growth of the Cu buffer along the [001] direction with the Cu cubic axes rotated in plane by 45° with respect to the Si(001) principal axes.[1] RHEED was used to monitor the change in surface in-plane lattice constant during growth by using the streaks in the pattern to calculate the nearest-neighbor distances for the Ni and Cu layers. At a Cu buffer thickness of 600 Å, the NB was found to be ~0.4% larger than that of bulk Cu. The Ni layer was shown to grow with much improved epitaxy on thicker Cu buffer layers. O'Brien and Tonner[6] have observed that the normalized MCXD intensity for Ni/Cu(001) in the remanent state is constant for the Ni thickness range of 12–75 ML, implying that the moment per atom remains constant in this thickness range. This result contrasts with the MCXD measurements performed on our sample where the MCXD signal increased with thickness as discussed separately in Ref. 19. The main difference in the two systems is that O'Brien and Tonner used Cu single crystals as opposed to our Cu buffer layer on Si(001) substrates. RHEED measurements showed that the 600-Å Cu buffer was still not relaxed to the bulk Cu value, and so our Ni films are subjected to more strain than O'Brien and Tonner's in the ultrathin limit. From Fig. 4, the surface in-plane lattice constant of 30 Å Ni is very close to the bulk Cu value, suggesting that it is strongly strained. This contrasts with the case of Ni films grown on Cu(001) single-crystal substrates which are reported to exhibit coherent growth up to 10 ML (~17 Å) thickness followed by strain relaxation.[26] The additional Cu cap present in our samples and not in O'Brien and Tonner's could also contribute to the
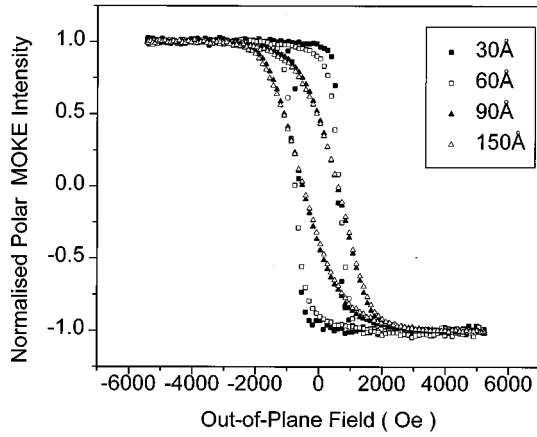
FIG. 5. Normalized polar MOKE hysteresis loops measured with an out-of-plane applied field for the wedge sample showing the reduction in perpendicular anisotropy with thickness from 30 to 150 Å Ni. The remanence is clearly reducing as the shape anisotropy forces the sample towards an in-plane easy axis.

differing amounts of strain in the two systems and hence to the difference in MCXD results for the two systems.

Polar MOKE measurements on the wedge sample (Fig. 5) revealed the changing anisotropy of the wedge sample from perpendicular towards in-plane easy axis at 150 Å. Figure 5 indicates that at 30 Å Ni coverage the polar MOKE loop has almost unity remanence, indicating an easy axis perpendicular to the film plane. Further Ni coverage up to 150 Å reduces the remanence progressively, with the loops tending towards a hard axis loop at higher Ni thicknesses.

V. CONTAMINATION, INTERMIXING, AND ROUGHNESS

It is most important to analyze in detail the possibility that the reduction in absolute moment per atom may be due to an extrinsic effect such as sample contamination or NiCu intermixing. PNR measures the average moment per atom over the thickness range of the magnetic layer, and so contamination would in effect ''dilute'' the amount of magnetic material in the Ni layer and lead to the observation of a reduced moment. Uniform contamination would affect the same volume fraction of all samples in a given growth environment and so could not explain the trend we have observed since the moment would be reduced by the same amount for each sample. The eight PNR samples, however, were grown under different conditions and thus under environments of different contamination levels. This cannot be the cause since we observe exactly the same trend of moment versus thickness for the MCXD wedge sample. In an attempt to explain the trend in moments for the PNR data, we can assume that there is a 23-Å ''magnetically dead'' layer in each sample. The dotted line in Fig. 4 shows the behavior corresponding to this hypothetical model. Apart from samples 5 and 6, the model yields a reasonable approximation to the values of average moment versus thickness data obtained from the previous analysis, and so it is important to now carefully consider the possibility of such a magnetically dead layer. We have considered two possible causes of a magnetically dead layer: (i) NiCu intermixing at the interfaces and (ii) oxygen and carbon contamination at the interfaces. The latter two

were the only significant contaminants observed by AES.

It is known from the Slater-Pauling curve,[27] which gives the net magnetic moment per atom as a function of the number of $3d$ electrons per atom, that a reduction in magnetic moment per atom will occur for various intra-$3d$ alloys. NiCu forms a simple solid solution in the bulk alloy over the entire range of composition. The addition of Cu to Ni has the effect of diluting the magnetic properties of the alloy such as saturation magnetization. Cu also causes a linear decrease in the Curie temperature from 63 K at 0% Cu, vanishing to 0 K at 62% Cu. A linear decrease of the moment results, from $0.6\mu_B$ in pure Ni to $0\mu_B$ at 62% Cu.[28,29] To create a 23-Å magnetically dead layer at room temperature, we would need 33% Cu intermixing over this length scale at the Ni/Cu interface/interfaces assuming the behavior of the bulk alloy. However, at room temperature there is layer-by-layer growth for Cu/Ni(001),[30,31] Ni/Cu(001),[4] and Ni/Cu(001)/Si(001).[32] It is therefore unlikely that NiCu intermixing is the mechanism responsible for the decreasing moment. This view is supported by our Auger spectroscopy studies.[19]

The worst contamination levels recorded in any sample by AES indicated a 4% oxygen component for the completed 600-Å Cu buffer and Ni layer. May has found that 0.5 ML of atomic oxygen suppresses the magnetization corresponding to one layer of Ni, and for 1.5 ML no ferromagnetic response from a 4-ML Ni film was found at 38 K.[33] Tischer et al. also find effects of similar magnitudes in their ultrathin Ni films.[34] The information depth of the Auger was approximately 10 Å. If we assume that the 4% O component is entirely on the surface, then there would be no more than 0.2 ML of oxygen on the surface. This oxygen would then combine with the growing Ni to form about 0.4 ML of NiO. It seems very unlikely that such a small NiO layer could destroy the magnetism of 23 Å of magnetic material. Furthermore, RHEED measurements after Ni growth do not show any evidence of a NiO layer which has a much larger lattice constant ($a_0 = 4.16$ Å) than Ni and so should have been visible. A carbon component was also present on the Si substrate, but the formation of an ordered Ni-C compound at the NiCu interface was not supported by RHEED. Carbon segregation to the surface of the Cu or Ni at room temperature is also ruled out by earlier work.[35]

PNR provides a further test of the hypothetical ''dead layer'' model shown in Fig. 4 since PNR is sensitive to the magnetic moment profile in the Ni layer. Figure 6 shows the result of a series of PNR simulations compared with the experimental data of sample 2, each incorporating a magnetically ''dead'' region within the Ni layer. Exactly the same parameters as obtained in the best fit for sample 2 [see Table I and Fig. 2(a)] were used in the simulations, except that the Ni layer was modeled in such a way so as to take into account a possible magnetically dead layer. Each of the modeled Ni layers in Fig. 6 has an average effect of 53 Å Ni with a magnetic moment per atom of $0.25\mu_B$, i.e., exactly equivalent to the best-fit parameters obtained for sample 2 assuming a homogeneous Ni layer of reduced moment. Figure 6(a) assumes a model with a magnetically dead layer extending from the Cu-cap/Ni-layer interface. Figure 6(b) assumes a model with a magnetically dead region extending from the Cu-buffer/Ni-layer interface. Finally, and perhaps more real-
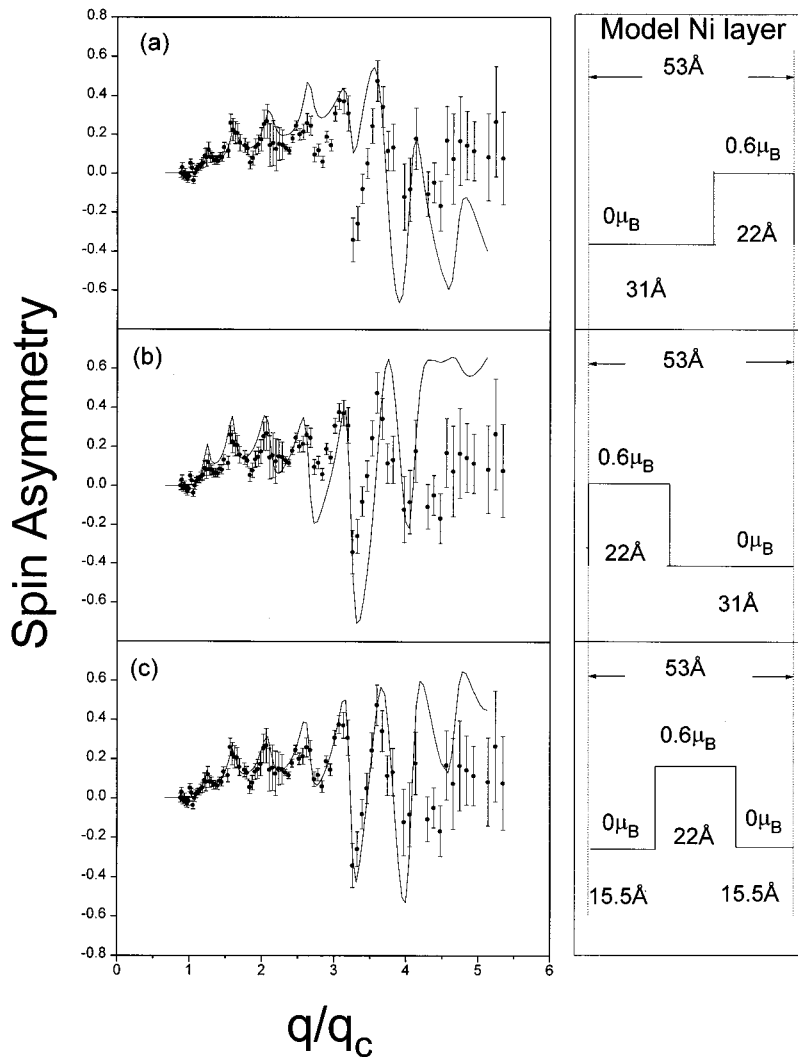
FIG. 6. PNR spin asymmetry simulations compared with the experimental spin asymmetry data of sample 2. (a) The Ni layer is modeled with a magnetically dead region extending from the Cu-cap/Ni-layer interface. (b) The Ni layer is modeled with a magnetically dead region extending from the Cu-buffer/Ni-interface. (c) The Ni layer is modeled with two magnetically dead regions extending from each Ni/Cu interface with a central magnetically alive region of bulk moment. The average effect of each model is a 53-Å Ni layer of moment $0.25\mu_B$. See the discussion in the main text.

istically, Fig. 6(c) models the sample with the Ni layer composed of two magnetically dead regions extending from each Ni/Cu interface and a central magnetically "alive" region of bulk magnetic moment. It is clear that each of the simulations give a poor fit to the experimental data above about (3–4) q_c. This is in sharp contrast to the excellent fit for sample 2 given in Fig. 2(a), assuming no magnetically dead layers, and highlights the capability of PNR in resolving the magnetic moment profile within a magnetic thin film. Attempts to fit the experimental data using models incorporating NiCu alloy regions with reduced moments were similarly unsuccessful. Therefore, we can find no evidence to suggest that sample contamination or NiCu intermixing is the mechanism responsible for the reduction in magnetic moment due to the formation of a magnetically dead layer.

Interface roughness gives rise to an effective perpendicular anisotropy[36] and also increases the surface area of the film resulting in an increase of contact area between the Ni and Cu layers in our system. Since the Ni atoms at a Ni/Cu interface are calculated to have a reduced moment of $0.39\mu_B$,[37] columnar growth of our thinnest samples could, if present, explain both the reduction in magnetic moment and the perpendicular magnetic anisotropy found in the Cu/Ni/Cu/Si(001) system. If interface roughness is solely re-

sponsible for the PMA in our thinnest films, then the correlation length of the roughness would have to be smaller than or comparable to the thickness of the film. But for our 30-Å Ni sample, this implies that the correlation length of the roughness is comparable to the wavelength of the incident neutrons ($\lambda \sim 10$ Å). This cannot be true, since to measure well-defined reflectivity oscillations with PNR the interface must be flat over a length scale much greater than the neutron wavelength; otherwise, the diffuse scattering is so large we cannot collect meaningful data. Therefore, our thinnest films cannot be columnar on the lateral scale required. However, we cannot rule out the possibility that large amplitude interface roughness with a correlation length much larger than λ could contribute to the moment reductions we observe.

VI. VOLUME DEPENDENCE OF THE MAGNETIC MOMENT

The presence or absence of magnetism in transition metals is determined by a competition between intra-atomic exchange interactions and interatomic electron motion, as has been discussed by Moruzzi and Marcus.[38,39] Since the interatomic motion depends strongly on the interatomic separa-

tion and because the *d* bands are partially filled, transition metals can be expected to be magnetic at sufficiently large volumes (low densities) and nonmagnetic at sufficiently low volumes (high densities). It is well known that ultrathin Ni grown on the Cu(001) surface undergoes a lattice expansion of 2.5% in plane to match that of the Cu seed layer, inducing a contraction of the perpendicular lattice spacing. The unit cell volume can therefore change during this strained growth. We can estimate the unit cell volume for 30 Å Ni growth (sample 1). Chang[3] used x-ray diffraction measurements to directly measure the perpendicular lattice spacing on a very similar system to our own: Cu(1000 Å)/Ni/Cu(1000 Å)/Si (001). Using the in-plane value of the lattice constant for 30 Å Ni (which was found to be almost the bulk Cu value) as measured by our RHEED and Chang's value for the perpendicular component for ultrathin Ni below 50 Å, we estimate the unit cell volume for 30 Å Ni to be expanded by approximately 2.6%. This is just a rough estimate, but is helpful in the following discussion.

It is reasonable to expect that the increased distance between the Ni atoms might cause band narrowing, changing the number of holes in the spin-up and spin-down bands, thereby changing the magnetic moment. Marcus and Moruzzi have calculated magnetic moment versus volume curves using spin-polarized total energy band calculations for various transition metals including fcc Ni.[7] The theoretical calculations are based on isotropic changes of volume of the Wigner-Seitz unit cell of atoms. They find that fcc Ni is a stable ferromagnet throughout the volume range studied. Their calculations show that an expanded volume gives an enhanced moment and a reduced volume gives a reduced moment. For fcc Ni it is a very weak effect, with a 1% change in volume corresponding to approximately 1% change in magnetic moment per atom. Therefore, the predictions of Marcus and Moruzzi would imply that sample 1 (30 Å Ni) should display only a slightly enhanced moment (2.6%) and not the dramatically reduced moment we observe. However, their calculations do show that a sharp transition does occur for bcc Ni from a nonmagnetic phase to approximately the bulk moment over a volume change of only 1% or so.[7] There is no evidence to support this growth mode from the literature or from our RHEED data. The sharp moment versus volume transition for bcc Ni occurs at a lattice spacing of $a_0 = 2.78$ Å,[40] whereas our RHEED data give $a_0 = 3.605$ Å. However, bcc can be regarded as a distorted fcc structure—i.e., fct where the c/a ratio is $\sqrt{2}$ for fcc. The PNR measurements are inconsistent with the predictions of Marcus and Moruzzi for fcc Ni in the bulk phase. Although we have clearly demonstrated that there is a strong correlation between the strain-induced anisotropic distortion of the Ni unit cell volume and the strongly reduced moments found in our fct structures, the currently available theoretical computations based on this anisotropic distortion indicate that the direct effect of strain cannot readily account for the observed reductions.[41] Further computational studies which take into account the specifics of the film structure would clearly be helpful in this context.

VII. CURIE TEMPERATURE

The variation of Curie temperature as a function of Ni thickness in the Ni/Cu(001) system has already been exten-

TABLE II. SQUID measurements of a sample with nominal structure 50 Å Cu/30 Å Ni/600 Å Cu/Si(001). The magnetization of the Ni is reduced by 14 ± 5 % as the temperature is increased from 50 to 300 K. This reduction is far too small to account for the reduction in moment for 30 Å Ni (83 ± 15 %) as measured by PNR.

Temperature (K)	Sample moment M (emu$\times 10^{-5}$)	$M/M_{50\,K}$
50	4.36 ± 0.19	1
200	4.03 ± 0.19	0.92
300	3.75 ± 0.12	0.86

sively studied.[6,42] The Curie temperature drops below room temperature for thin films below about 5 ML and rises to 550 K for 16.0 ML (28 Å). Since the thinnest Ni film studied here is 30 Å, we can expect that our measurements at room temperature are well below T_c for all of our samples. However, the literature[6,42] refers to Ni grown on Cu(001) single crystals and not Ni grown on Cu/Si(001) as studied here. Consequently, using a SQUID magnetometer, we have investigated the temperature dependence of the magnetization of an additional sample specially prepared for this study. The nominal structure of the sample was 50 Å Cu/30 Å Ni/600 Å Cu/Si(001), but we emphasize that this should not be confused with sample 1 (30 Å Ni) listed in Table I. Table II shows the results of this measurement performed at three different temperatures 50, 200, and 300 K. Table II shows that the magnetization is reduced by $14\% \pm 5\%$ as we increase the temperature from 50 to 300 K. From Table I the reduction in moment per atom for sample 1 (30 Å Ni thickness) as measured by PNR is $83\% \pm 15\%$, and so this strong reduction cannot be a consequence of a reduction in Curie temperature due to the small 30 Å Ni thickness. Since the Curie temperature increases as the Ni thickness increases, we can expect that the reduction in moment due to the Curie temperature effect for the thicker Ni films will be less than 14%. Although it is clear that the reduction in Curie temperature with decreasing Ni thickness can contribute to the reduction in moment we observe, the effect is far too small to account for the experimental data and therefore we can find no evidence to suggest that this is the mechanism responsible for the strongly reduced moments.

VIII. CONCLUSIONS

The thickness dependence of the magnetic moment per atom in the Cu/Ni/Cu/Si(001) system has been studied using polarized neutron reflection. In all samples a uniform magnetization model fits the data very well. We find a dramatic reduction in the moment per atom below 100 Å in agreement with AGFM measurements performed on the same samples. MCXD measurements on a wedge sample show exactly the same trend in $\langle L_z \rangle$ and $\langle S_z \rangle$ and total moment versus nominal thickness, as the PNR and AGFM versus PNR determined magnetic thickness. We find that there is a strong correlation between the increasing strain measured by RHEED and the reduction in moment per atom. Our results differ from those of O'Brien and Tonner[6] who observed that the normalized MCXD intensity for Ni/Cu(001) in the remanent state is constant for Ni in the thickness range 12–75

ML. We attribute the different behavior for the two systems to the different degrees of strain in the systems due to the different substrates and overlayers. The additional Cu capping layer present in our samples significantly adds to the strain in the Ni layer, and therefore a reduced moment is seen at comparatively large Ni thickness. We find our results cannot be explained by sample contamination or NiCu intermixing, but are inconsistent with the predictions of Marcus and Moruzzi for isotropically expanded bulk fcc Ni. Although thermal effects contribute to the reduction in moments we observe with respect to the bulk ground-state value, temperature-dependent SQUID measurements show the effect is far too small to account for the total reduction in moments as measured by PNR. We cannot rule out the possibility that large amplitude interface roughness with a correlation length much larger than the neutron wavelength could contribute to the moment reductions we observe. Further work is underway to study the variation in moment per atom for a fixed Ni thickness layer as a function of Cu buffer thickness. The surprisingly large thickness range over which the perpendicular anisotropy exists in the Cu/Ni/Cu/Si(001) system may be in part due to the reduced moment per Ni

atom we have found below 100 Å. Since the moment is greatly reduced below 100 Å, it will require a relatively thick Ni film before the shape anisotropy is able to win over the magnetoelastic perpendicular anisotropy. We suggest that the strain-induced anisotropic change in volume of the Ni unit cell below 100 Å Ni thickness is correlated with the large variation in the magnetic moment per atom. However, the currently available theoretical calculations[41] indicate that the direct effect of strain cannot readily account for the observed moment reductions, and so further computational studies which take into account the specifics of the film structure would be desirable.

[1] R. Naik, C. Kota, J. S. Payson, and G. L. Dunifer, Phys. Rev. B **48**, 1008 (1993).

[2] R. Naik, A. Poli, D. McKague, A. Lukaszew, and L. E. Wenger, Phys. Rev. B **51**, 3549 (1995).

[3] Chin-An Chang, J. Appl. Phys. **68**, 4873 (1990).

[4] R. Jungblut, M. T. Johnson, J.aan de Stegge, A. Reinders, and F. J. A. den Broeder, J. Appl. Phys. **75**, 6424 (1994).

[5] Gabriel Bochi, H. J. Hug, D. I. Paul, B. Stiefel, A. Moser, I. Parashikov, H. J. Guntherodt, and R. C. O'Handley, Phys. Rev. Lett. **75**, 1839 (1995).

[6] W. L. O'Brien and B. P. Tonner, Phys. Rev. B **49**, 15 370 (1994).

[7] P. M. Marcus, V. L. Moruzzi, and K. Schwarz, in *Computer-Based Microscopic Description of the Structure and Properties of Materials*, edited by J. Broughton, W. Krakow, and S. T. Pantelides, MRS Symposia Proceedings No. 63 (Materials Research Society, Pittsburgh, 1986), p. 117.

[8] C. L. Fu, A. J. Freeman, and T. Oguchi, Phys. Rev. Lett. **54**, 2700 (1985).

[9] R. Richter, J. G. Gay, and J. R. Smith, Phys. Rev. Lett. **54**, 2704 (1985).

[10] C. L. Fu, A. J. Freeman, and T. Ogochi, Phys. Rev. Lett. **54**, 2700 (1985).

[11] O. Hjortstam, J. Trygg, J. M. Wils, B. Johansson, and O. Eriksson, Phys. Rev. B **48**, 9204 (1996).

[12] Y. Wu, J. Stohr, B. D. Hermsmeier, M. G. Samant, and D. Weller, Phys. Rev. Lett. **69**, 2307 (1992).

[13] G. H. Daalderop, P. J. Kelly, and M. F. H. Schuurmans, Phys. Rev. B **44**, 12 054 (1991).

[14] S. J. Blundell and J. A. C. Bland, Phys. Rev. B **46**, 3391 (1992).

[15] *Polarised Neutron Reflection*, edited by J. A. C. Bland, Vol. I of *Ultrathin Magnetic Structures* (Springer-Verlag, Berlin, 1994), pp. 305–342.

[16] J. A. C. Bland, A. D. Johnson, H. J. Lauter, R. D. Bateson, S. J. Blundell, C. Shackleton, and J. Penfold, J. Magn. Magn. Mater. **93**, 513 (1991).

[17] S. J. Blundell and J. A. C. Bland, J. Magn. Magn. Mater. **121**, 185 (1993).

[18] R. Felci, J. Penfold, R. C. Ward, and W. G. Williams, Appl. Phys. A **45**, 169 (1988).

[19] J. Lee, G. Lauhoff, M. Tselepi, S. Hope, P. Rosenbusch, J. A. C. Bland, H. A. Oürr, G. van der Laan, J. Ph. Schillé, and J. A. D. Matthew (unpublished).

[20] J. R. Ives, R. J. Hicken, J. A. C. Bland, C. Daboo, M. Gester, and S. J. Gray, J. Appl. Phys. **75**, 6458 (1994).

[21] J. A. C. Bland, M. J. Padgett, R. J. Butcher, and N. Bett, J. Phys. E **22**, 308 (1989).

[22] L. Nevot and P. Croce, Rev. Phys. Appl. **15**, 761 (1980).

[23] Samples 6 and 8 were not measured with AGFM as they were both damaged in transit.

[24] B. T. Thole, P. Carra, F. Sette, and G. van der Laan, Phys. Rev. Lett. **68**, 1943 (1992).

[25] P. Carra, B. T. Thole, M. Altarelli, and X. Wang, Phys. Rev. Lett. **70**, 694 (1993).

[26] J. Zhang, Z. L. Han, S. Varma, and B. P. Tonner, Surf. Sci. **298**, 351 (1993).

[27] D. Jiles, *Introduction to Magnetism and Magnetic Materials* (Chapman & Hall, London, 1991).

[28] D. C. Jiles, T. T. Chang, D. R. Hougan, and R. Ranjan, J. Appl. Phys. **64**, 362 (1988).

[29] Hong Huang, Xue-Yuan Zhu, and J. Hermanson, Phys. Rev. B **29**, 2270 (1984).

[30] A. Chambers and D. C. Jackson, Philos. Mag. **31**, 1357 (1975).

[31] J. Shen, J. Giergiel, and J. Kirschner, Phys. Rev. B **52**, 8454 (1995).

[32] R. Naik, M. Ahmed, G. L. Dunifer, C. Kota, A. Poli, Ke Fang, U. Rao, and J. S. Payson, J. Magn. Magn. Mater. **121**, 60 (1993).

[33] F. May, M. Tischer, D. Arvanitis, M. Russo, J. Hunter Dunn, H. Henneken, H. Wende, R. Chauvistre, N. Martensson, and K. Barberschke, Phys. Rev. B **53**, 1076 (1994).

[34] M. Tischer, D. Arvanitis, T. Yyokoyama, T. Ledorer, L. Troger,

and K. Baberschke, Surf. Sci. **307−309**, 1096 (1984).

[35] J. M. Blakely, J. S. Kim, and H. C. Potter, J. Appl. Phys. **41**, 2693 (1970).

[36] P. Bruno, J. Appl. Phys. **64**, 3153 (1988).

[37] Ding-sheng Wang, A. J. Freeman, and H. Krakauer, Phys. Rev. B **26**, 1340 (1982).

[38] V. L. Moruzzi, Phys. Rev. Lett. **57**, 2211 (1986).

[39] V. L. Moruzzi and P. M. Marcus, Phys. Rev. B **34**, 1784 (1986).

[40] P. M. Marcus and V. L. Moruzzi, J. Appl. Phys. **63**, 4045 (1988).

[41] G. Guo (unpublished).

[42] F. Huang, M. T. Kief, G. J. Mankey, and R. F. Willis, Phys. Rev. B **49**, 3962 (1994).